Vietnam Journal of Science and Technology ***63*** *(2) (2025)*

doi.10.15625/2525-2518/17630

Production of porous material from solar panels waste glass

Bui Khac Thach[1, 2], Truong Vu[1, 2], Do Quang Minh[1, 2, *], Ly Cam Hung[3], Phan Dinh Tuan[3, 4]

[1]*Faculty of Materials Technology, Ho Chi Minh City University of Technology, 268 Ly Thuong Kiet St., Ward 14, District 10, Ho Chi Minh City, Viet Nam*

[2]*Vietnam National University Ho Chi Minh City, Linh Trung Ward, Thu Duc District, Ho Chi Minh City, Viet Nam*

[3]*Hochiminh City University of Natural Resources and Environment, 236B Le Van Sy St., Tan Binh District, Ho Chi Minh City, Viet Nam*

[4]*Applied Research Institute of Natural Resources, Materials and Environment, 58/4 Tran Van Du St., Tan Binh District, Ho Chi Minh City, Viet Nam*

[*]Email: *mnh_doquang@hcmut.edu.vn*

Received: 3 November 2022; Accepted for publication: 5 March 2025

Abstract. Porous material presents itself as a viable solution for recycling waste photovoltaic panels. In this study, the feasibility of utilizing waste solar panel glass to produce porous material was assessed by incorporating 10 weight percent (wt.%) $CaCO_3$ and 10 wt.% water glass. A simulation of heating microscope method was utilized to determine the firing temperature for the porous material, ranging from 830 °C to 910 °C. The sintered samples have the specific volumetric density ranging from 0.40 to 0.43 g/cm^3, water absorption ranging from 171.1 to 202.7 wt.% and apparent porosity of 76.1 to 78.2 %. The morphology of the porous material samples fired at various temperatures demonstrates that the pores' structure is interconnected. The X-Ray Diffraction (XRD) patterns show that the porous material contains a glassy phase and an impurity one like Devitrite. The findings show that the porous glass not only holds water well, but it is also easy to be re-wetted. Therefore, the porous glass exhibits potential for use as a water-retaining medium, finding applications in various fields, including hydroponics and aquaponics.

Keywords: heating microscope, porous material, waste glass from solar panels.

Classification numbers: 2.9.2, 2.10.3

1. INTRODUCTION

Solar energy is estimated to reach 4500 GW by 2050. With the average lifetime of a photovoltaic (PV) panel of 25 years, the global waste PV panels are predicted to reach 4 – 14

million tons by 2030, and up to 78 million tons by 2050 [1]. The disposal and treatment request for the waste PV panels will become the global severe problem in the next decades.

The utilization of porous glass material presents an effective solution for managing waste glass from solar cells. This material is formed by fusing molten glass powder into a stable framework, with the pores created through the addition of a gas-generating decomposer. Notably, porous material exhibits high porosity, low thermal conductivity, chemical stability, water resistance, and non-combustibility, making it a desirable option for various applications. Typically, the firing temperature for porous materials ranges from 700 to 900 °C [2,3]. Foaming agents can be classified into two categories: gaseous decomposers, such as calcium carbonate ($CaCO_3$) [4], or gaseous combustibles, such as carbon (C), silicon carbide (SiC) [5], etc.

The porous glass finds diverse applications in various fields, including serving as a filter media for removing phosphorus-containing particulate matter in municipal wastewater [6], highly suitable as a substrate in hydroponic and aquaponic systems [7]. In addition, it is also used as material for insulation, electromagnetic absorption, lightweight building materials [8] etc. Waste glass from solar panels after separation from photovoltaic modules is highly non-recyclable as glass raw material for its impurities. The cleaning process for the used glass in solar panels is time, chemicals consuming and hence expensive [9,10]. Utilizing waste glass from solar panels in the production of ceramics is considered a reasonable approach, including fired clay bricks [11], geopolymers [12], glass ceramics [13], aggregates for composite cements [14, 15], etc.

It is technically important to determine the firing temperatures for making porous material. If the heating temperature is too high, a large amount of heat is undesirably consumed. Moreover, the liquid glass will seal off the pores, diminishing the firing efficiency. If the calcination temperature is too low, no bonds will be formed between the glass particles to form the structural framework. By the way, it is necessary to retain its mechanical strength while keeping high porosity of the material. Therefore, it is essential to ensure that the firing temperature is in accordance with the temperatures at which the foaming agents undergo decomposition [16].

The thermodynamic characteristics of glass, such as the glass formation temperature (Tg), conventionally defined as the temperature corresponding to the viscosity of 1013 Poises, can be obtained using either Differential Thermal Analysis (DTA) or Differential Scanning Calorimetry (DSC) thermal analytical techniques [17]. Nevertheless, the waste glass does not possess a distinct melting point; instead, it undergoes a gradual transformation from a solid state to a liquid state across the range of softening temperatures. The firing temperature of the foam material can be selected within the temperature range determined by a Heating Microscopy (HM) [18]. Observation of deformation when heating cylindrical glass samples with height (H) equal to width (D), and H = D = 6mm, temperature rise rate of 10 °C/min. As per DIN 51730 (1998) / ISO 540 (2008) [19, 20], the typical glass temperatures are determined in the following manner:

- Sintering temperature (T_{sinter}): the sample undergoes a 5 %-dimensional shift compared to the initial image.

- Softening temperature (T_s): rounded edges start to become observable (usually H = ¾ H_0).

- Sphere temperature: the sample takes on a spherical appearance (H =D).

- Hemisphere temperature: the height of the sample is equal to half of the diameter (H = 1/2D).

- Flow temperature (T_f): the sample is melted, resulting in a reduction of its initial height to one-third ($H = 1/3H_0$).

The softening temperature range (ΔT) is defined as the difference between the flow temperature (T_f) and the softening temperature (T_s)

In this work, the softening temperature range of glass samples extracted from waste solar panels was determined by simulating the HM technique. Digital camera images were analyzed to ascertain this range. Subsequently, the calcination temperatures for the foam glass samples were chosen within the softening temperature range of the glass. This choice ensured compatibility with the decomposition temperature of $CaCO_3$, enabling the formation of pores in the foam glass. The mechanical and physical properties of the samples calcined at different temperatures, such as porosity, compressive strength, water absorption, and structural properties, were determined to provide data for the selection of materials with known properties.

2. MATERIALS AND METHODS

2.1. Materials

Waste photovoltaic panels were obtained from Solar Vietnam Joint Stock Company, Viet Nam. The glass component was physically separated from the layers of ethylene vinyl acetate (EVA) binder, aluminum ribbon, and other components by applying a flame using a heat gun to the surface of the solar panels. The waste glass was then subjected to grinding in a ball mill for 6 hours and sieved through a 125 µm mesh to eliminate any EVA residue. Commercial $CaCO_3$ powder (Vietnam, >99 %) was employed as a foaming agent and sodium water glass (New Ha Viet Silicate, Vietnam, >96 %) served as a binder. The chemical composition and the mean size of the raw materials was analyzed in our previous study [16], revealing the oxide composition (wt.%) of the used waste glass is: SiO_2 - 67.17, Na_2O - 12.74, CaO - 11.74, Al_2O_3 – 2.00, Fe_2O_3 - 1.92, MgO - 2.43, Others - 1.44, loss on ignition (LOI) - 0.56; and for calcium carbonate: CaO - 56.28, Fe_2O_3 - 0.01, MgO - 0.32, Others - 0.01, LOI - 43.38; and water glass: SiO_2 - 69.15, Na_2O - 27.82, CaO - 0.4, Al_2O_3 - 1.66, Fe_2O_3 - 0.07, Others - 0.90. The mean particle size (d50) of the waste glass obtained from used solar panels and the $CaCO_3$ powder was recorded as 35.0 µm and 18.1 µm, respectively.

2.2. Methods

2.2.1. Characteristic temperatures

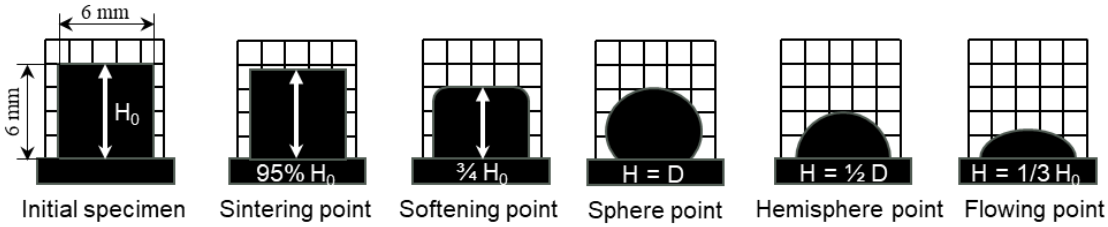

Figure 1. Schematic illustration of the characteristic points and their appearance of the specimen during the heating process.

A cylindrical specimen of glass powder, measuring 6 × 6 mm, was compressed and placed

inside a furnace with a heating rate of 10 °C/min. The entire transformation of sample's shape and size was monitored using a Canon 700D digital image camera with a Canon 50mm f/1.8 STM lens. The images were analyzed based on the measurement of and comparison with the height of the green sample during heating with the use of ImageJ software to determine the characteristic temperatures in the heating process (Fig. 1).

2.2.2. Physical characteristics

To create an aggregated heap, the raw materials are combined with 10 wt.% calcium carbonate ($CaCO_3$) and 10 wt.% water glass, based on the weight of the waste glass powder. Additionally, water is incorporated in a fixed proportion of 20 wt.% by weight of solids to ensure that all the components can effectively form the desired aggregated heap [21]. The heap is well-mixed in a whisk for 5 min, then shaped in a PVC mold with height H = 12 mm, and diameter Φ = 18 mm. After forming, the samples were dried in a dryer (Venticell) at 110 °C for 2 h. Then, samples were fired in an electric kiln at a heating rate of 10 °C/min, with a soaking time of 15 min. The firing temperatures were chosen based on the simulation of the HM technique.

Volumetric density, water absorption, and apparent porosity: The parameters were established in accordance with ASTM C20-00 (2022) [22]. Specifically,

Volumetric density (ρ):

$$\rho = \frac{D}{W - S}\ (g/cm^3) \tag{1}$$

Water absorption:

$$A_w = \frac{W - D}{D}\ (\%) \tag{2}$$

Apparent porosity:

$$\varepsilon_{ap} = \frac{W - D}{W - S}\ (\%) \tag{3}$$

with, D: dry weight of the sample (g);

S: place the test sample in water and boil for 2 h and then determine the weight suspended in water using hydrostatic weighing (g)

W: after determining the suspended weight, lightly blot each sample with a moistened smooth linen to remove all liquid drops and determine the saturated weight (g)

Total porosity (ε) is calculated using the volumetric density (ρ) and the density of the sintered powder (ρ_t), as per the following equation:

$$\varepsilon = 1 - \frac{\rho}{\rho_t}\ (\%) \tag{4}$$

The ρ_t was determined by water pycnometer, with the calculation as follows:

$$\rho_t = \frac{M_2 - M_1}{(M_4 - M_1) - (M_3 - M_2)}\ (g/cm^3) \tag{5}$$

with, M_1: weight of the pycnometer (g);

M_2: weight of the pycnometer and dried powder (g);

M_3: weight of the pycnometer, dried powder, and filled water (g);

M_4: weight of the pycnometer and filled water (g).

Compressive strength of porous glass: After the firing process, the samples were ground and formed into cylindrical shapes with dimensions of 15 mm in height and 30 mm in diameter. Subsequently, the compressive strength of the samples was evaluated using the DTU-900MH (Daekyung Tech, Korea) with a loading rate of 1.5 kN/min. Figure 2 illustrates the compressive strength test.

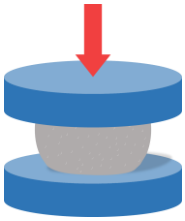

Figure 2. Experimental setup for the compressive strength test conducted on porous-glass samples.

Water retention: The sintered samples underwent a 4-hour boiling process in hot water, followed by room temperature curing and drying at 110 °C. The mass loss of the samples was determined by weighing them at different intervals during the curing time.

2.2.3. Microstructure and morphology analyses:

The phase composition of the calcined samples was determined by XRD using a PHASER D2 diffractometer (Bruker, Germany) with Cu-Kα radiation and a 2θ scanning range of 5° to 80°, with a 0.02° step. The ICDD PDF-2 database was used to determine phase composition.

A digital microscope with a maximum magnification of 1600x (China) was used to analyze the pore morphology of sintered samples.

3. RESULTS AND DISCUSSIONS

3.1. Foaming process investigation

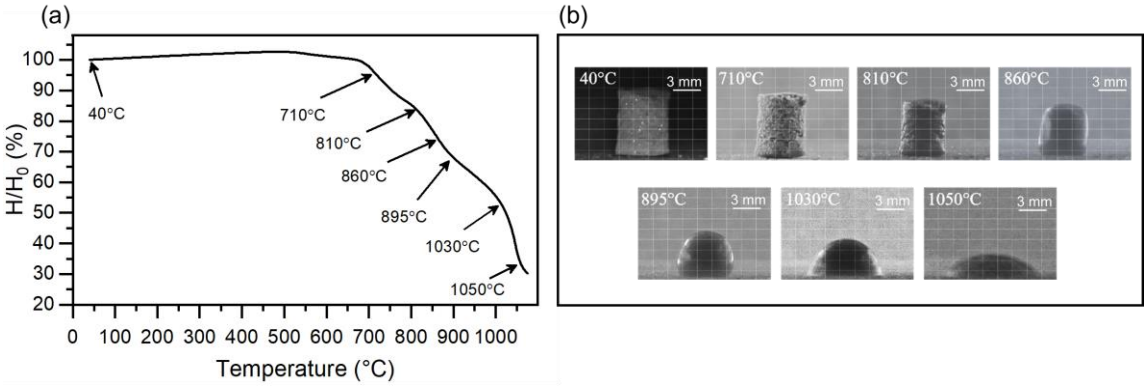

Figure 3. (a) Specimen height change during heating and (b) typical changes in glass specimen shapes during heating in an electric kiln.

Figure 3a illustrates the variation in sample height during the heating process. Sintering began at 710 °C. As the temperature increased, the softening temperature of the sample was observed at 860 °C. Concurrently, the sample height decreased by approximately 75 % compared to its initial height. However, during image analysis, it was observed that the sample exhibited edge rounding at 810 °C (Fig. 3b). At 895 °C, the sample transformed into an almost spherical shape. Subsequently, at higher temperatures, the sample exhibited a hemisphere shape at 1030 °C and a flowing state at 1050 °C.

Based on the obtained results, the softening temperature range of the waste glass powder was determined to be from 810 °C to 1050 °C. Considering the behavioral characterization of the samples, firing temperatures were selected within this softening temperature range. The range of firing temperatures is from the lowest value (830 °C) to the highest value (910 °C), with a consistent increment of 20 °C between each temperature point. The samples were subjected to a heating rate of 10 °C/min and held at the respective firing temperatures for a duration of 15 min in an electrical kiln.

3.2. Physical and mechanical properties

The relationships of volumetric density, total porosity, and compressive strength are shown in Fig. 4a. When the firing temperature was between 830 – 870 °C, the volumetric density was decreased from 0.42 to 0.40 g/cm^3 and the compressive strength was decreased from 0.79 to 0.59 MPa while the total porosity was increased from 82.0 to 83.9 %. At higher firing temperatures, up to 910 °C, the volumetric density and the compressive strength were increased to 0.43 g/cm^3 and 0.85 MPa, respectively. In addition, the total porosity was reduced to 81.8 %.

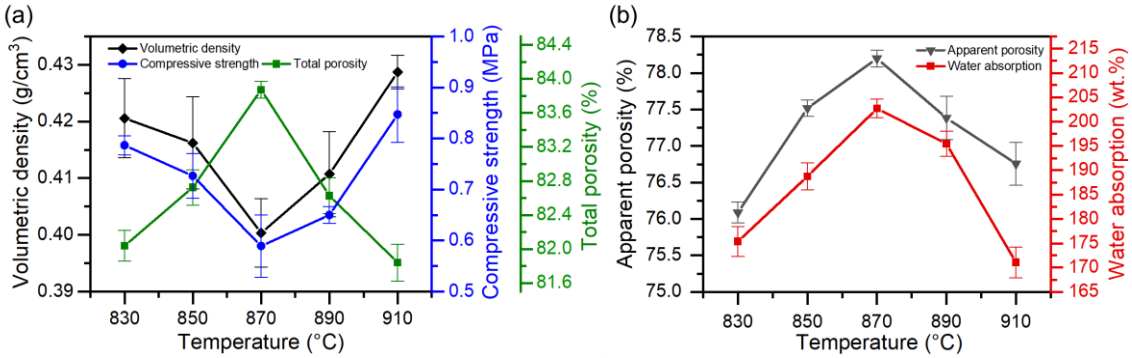

Figure 4. The correlation between (a) volumetric density, compressive strength, and total porosity and b) apparent porosity and water absorption.

As the open porosity increased, the water absorption also increased (Fig. 4b). Samples calcined at 870 °C had the maximum water absorption (202.7 wt.%) and the highest apparent porosity (78.2 %). Based on the findings, the optimal calcination temperature for achieving maximum water absorption was determined to be 870 °C. In addition, it was observed that at higher temperatures, specifically at 910 °C, the interconnecting walls among the voids are expected to undergo deformation, leading to a reduction in apparent porosity.

3.3. Morphological properties

Figure 5 displays the morphology of the porous glass samples. The interconnected structure of the pores in the samples fired at different temperatures is readily apparent.

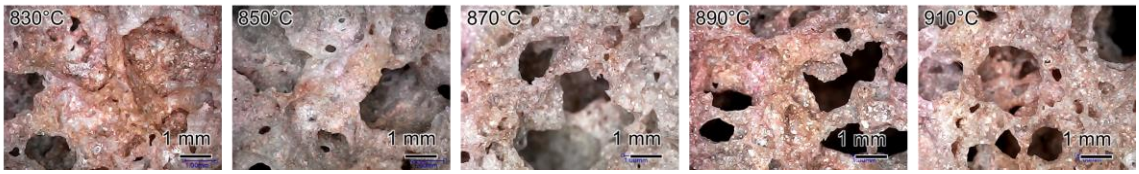

Figure 5. Morphology of porous glass samples at different firing temperatures.

The interior of all samples was heterogeneous due to the significant amount of gas produced from the decomposition of calcium carbonate. As a result, the pore wall began to break down and partially opened the pore [23, 24]. This has increased the water absorption capacity of the porous material.

3.4. Phase compositions of sintered samples

Figure 6a is the XRD pattern of samples fired in different temperatures compared to the XRD pattern of a dried sample.

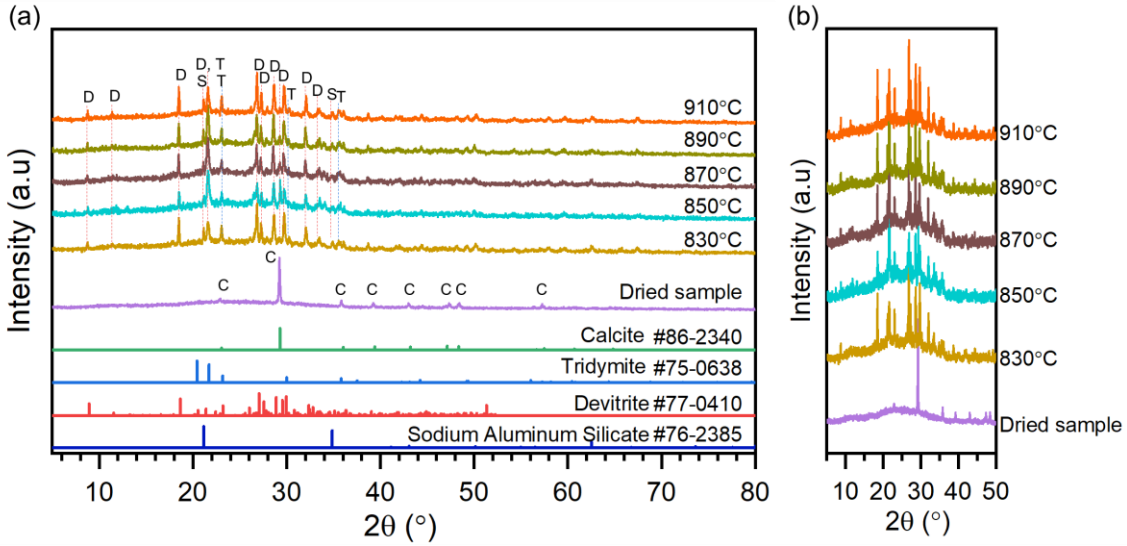

Figure 6. (a) XRD patterns and (b) the enlarged XRD patterns from 5 - 50° of porous glass samples that were fired at different temperatures.

The phase in the dried sample was $CaCO_3$ in the form of calcite (PDF #86-2340). The crystal phase compositions of all fired samples were tridymite (PDF #75-0638), Devitrite (PDF #77-0410) and sodium aluminum silicate (PDF #76-2385). The absence of $CaCO_3$ peaks in the sintered samples indicated that the $CaCO_3$ had completely decomposed at the high temperatures. Furthermore, there are no distinctive peaks indicative of the CaO phase resulting from the decomposition reaction of $CaCO_3$. The CaO product is an alkaline earth modifier oxide intended to dissolve and modify the glass network at high temperature [25, 26]. In the enlarged XRD patterns of porous glass materials (Fig. 6b), the broad peak around the diffraction angle 2θ from 20 - 30° indicates the glassy phase in the initial and fired samples. Devitrite crystals formed as an unwanted crystalline impurity during the glass soaking time [27].

3.5. Water retention ability

The water retention ability of sintered samples under room temperature and drying conditions is shown in Figure 7. Capillary pores are effective at water retention; smaller pores generate stronger capillary forces that keep water in the pore spaces and retain it for longer periods [28, 29]. Samples cured at room temperature could release almost all of the water only after 3 days, but samples dried at 110 °C could nearly completely discharge their water after 2 hours. The results indicate that the porous glass not only holds water well, but it is also simple to be re-wetted by drying. It is expected to have potential uses in hydroponic and aquaponic systems as a medium with water-retention properties.

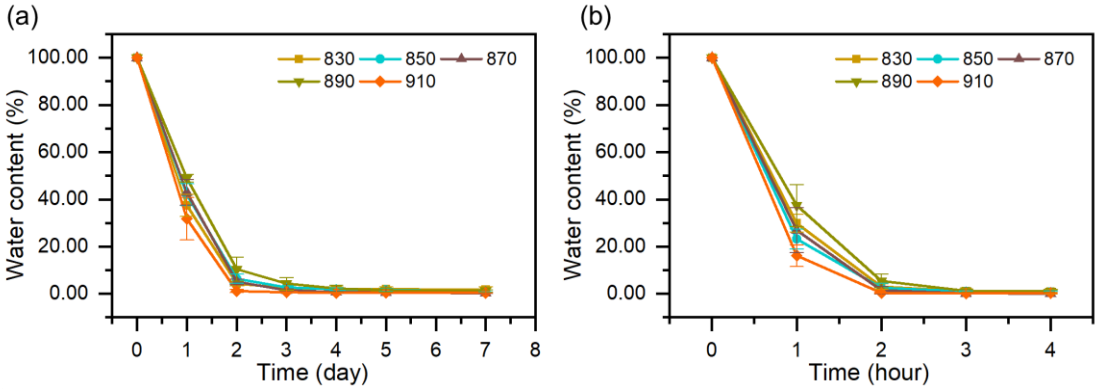

Figure 7. The water retention ability of sintered samples at (a) room temperature and (b) drier at 110 °C

4. CONCLUSION

The utilization of a mixture comprising glass powder derived from used solar panels, $CaCO_3$, and water glass allowed for the creation of diverse foam glass materials with varying porosity. The prototyping approach, involving a 10 wt.% water glass binder and utilization of a plastic mold for casting, demonstrated its suitability for producing these types of materials.

Images captured while the heating stage have been used to select the foaming temperature, enabling a tailored approach to attain desired physical and mechanical properties in the porous glass.

Under the specified conditions, the materials exhibited a volumetric density ranging from 0.40 to 0.43 g/cm^3 and a water absorption ranging from 171.1 to 202.7 wt.%, with firing temperatures between 830 °C and 910 °C and a $CaCO_3$ content of 10 wt.%.

The porous glass materials, characterized by an apparent porosity ranging from 76.1 % to 78.2 %, are well-suited for applications as water-retaining materials in hydroponic and aquaponic systems.

Acknowledgements. The authors acknowledge financial support from the Ministry of Natural Resources and Environment of Vietnam through the Project coded 04/HĐ-BQLTDA-tm.

CRediT authorship contribution statement. Bui Khac Thach: Investigation, Visualization, Writing - original draft. Truong Vu: Investigation. Do Quang Minh: Writing - review and editing, Supervision. Ly Cam Hung: Funding acquisition. Phan Dinh Tuan: Funding acquisition.

Declaration of competing interest. The authors declare that they have no known competing financial interests or personal relationships that could have appeared to influence the work reported in this paper.

REFERENCES

1. Chowdhury Md. S., Rahman K. S., Chowdhury T., Nuthammachot N., Techato K., Akhtaruzzaman Md., Tiong S. K., Sopian Sopian K., and Amin N. - An overview of solar photovoltaic panels' end-of-life material recycling. Energy Strategy Reviews **27** (2020) 100431. doi: 10.1016/j.esr.2019.100431.
2. Liu P. S., and Chen G. F. - Chapter Six - Applications of Porous Ceramics In: Liu P. S., and Chen G. F. (Eds.), Porous Materials, Boston, Butterworth-Heinemann, 2014, pp. 303-344. doi: 10.1016/B978-0-12-407788-1.00006-X
3. Mohammed Al-Saudi S. K., and Géber R. - Production of lightweight geopolymer concrete with foam glass aggregate derived from cathode-ray glass waste, Case Studies in Construction Materials **21** (2024) e03888. doi: 10.1016/j.cscm.2024.e03888.
4. Chen B., Wang K., Chen X., and Lu A. - Study of Foam Glass with High Content of Fly Ash Using Calcium Carbonate as Foaming Agent, Materials Letters **79** (2012) 263-265. doi: 10.1016/j.matlet.2012.04.052.
5. da Silva R. C., Puglieri F. N., de Genaro Chiroli D. M., Bartmeyer G. A., Kubaski E. T., and Tebcherani S. M. - Recycling of glass waste into foam glass boards: A comparison of cradle-to-gate life cycles of boards with different foaming agents, Science of the total Environment **771** (2021) 145276. doi: 10.1016/j.scitotenv.2021.145276.
6. Jeong T. U., Chu K. H., Kim S. J., Lee J., Chae K. J., and Hwang M. H. - Evaluation of foam-glass media in a high-rate filtration process for the removal of particulate matter containing phosphorus in municipal wastewater, Journal of Environmental Management **239** (2019) 159-166. doi: 10.1016/j.jenvman.2019.03.064.
7. Flood M., Fennessy L., Lockrey S., Avendano A., Glover J., Kandare E., and Bhat T. - Glass Fines: A review of cleaning and up-cycling possibilities, Journal of Cleaner Production,, **267** (2020) 121875. doi: 10.1016/j.jclepro.2020.121875.
8. Silva R. V., de Brito J., Lye C. Q., and Dhir R. K. - The role of glass waste in the production of ceramic-based products and other applications: A review, Journal of Cleaner Production **167** (2017) 346-364. doi: 10.1016/j.jclepro.2017.08.185.
9. Xu Y., Li J., Tan Q., Peters A. L., and Yang C. - Global status of recycling waste solar panels: A review, Waste Management **75** (2018) 450-458. doi: 10.1016/j.wasman. 2018.01.036.
10. Sanathi R., Banerjee S., and Bhowmik S. - A technical review of crystalline silicon photovoltaic module recycling, Solar Energy **281** (2024) 112869. doi:10.1016/ j.solener.2024.112869.
11. Lin K. L., Huang L. S., Shie J. L., Cheng C. J., Lee C. H., and Chang T. C. - Elucidating the effects of solar panel waste glass substitution on the physical and mechanical characteristics of clay bricks, Environmental Technology **34** (2013) 15-24. doi:10.1080/ 09593330.2012.679693.
12. Nguyen H. T., Nguyen Q. B., Nguyen V. P., and Pham T. K. - Syntheses and Characteristics of Calcium-Based Geopolymer from Solar-Cell Panel-Glass Waste by Hydrothermal Method, Materials and Technology **58** (2024) 467-475. doi: 10.17222/mit.2024.1153.

13. Lin K. L., Chu T. C., Cheng C. J., Lee C. H., Chang T. C., and Wang K. S. - Recycling solar panel waste glass sintered as glass-ceramics, Environmental Progress & Sustainable Energy **31** (2012) 612-618. doi: 10.1002/ep.10587.
14. Pavlopoulos C., Kelesi M., Michopoulos D., Papadopoulou K., Lymperopoulou T., Skaropoulou A., Tsivilis T., and Lyberatos G. - Management of end-of-life photovoltaic panels based on stabilization using Portland cement, Sustainable Chemistry and Pharmacy **27** (2022) 100687. doi: 10.1016/j.scp.2022.100687.
15. Zele S., Joshi A., Gogate N., Marathe D., and Shitole A. - Experimental investigation on utilization of crushed solar panel waste as sand replacement in concrete, Solar Energy **269** (2024) 112338. doi: 10.1016/j.solener.2024.112338.
16. Thach B. K., Tan L. N., Minh D. Q., Hung L. C., and Tuan P. D. - Production of Porous Glass-Foam Materials from Photovoltaic Panel Waste Glass In: Mohd Salleh M. A. A., Che Halin D. S., Abdul Razak K., and Ramli M. I. I. (Eds.), Proceedings of the Green Materials and Electronic Packaging Interconnect Technology Symposium, Singapore, Springer Nature, 2023, pp. 317-327. doi: 10.1007/978-981-19-9267-4_34
17. Mazurin O. V. - Problems of compatibility of the values of glass transition temperatures published in the world literature, Glass Physics and Chemistry **33** (2007) 22-36. doi:10.1134/S108765960701004X.
18. Venturelli C. - Heating Microscopy and its Applications, Microscopy Today **19** (2011) 20-25. doi: 10.1017/S1551929510001185.
19. DIN 51730, Determination of Fusibility of Fuel Ash, German Institute for Standardisation, 1998.
20. ISO 540:2008, Hard coal and coke - Determination of ash fusibility, International Organization for Standardization, 2008.
21. Thach B. K. - Study of manufacture of porous material-based waste solar panels, Viet Nam, 2022, (in Vietnamese).
22. ASTM C20-00, Standard Test Methods for Apparent Porosity, Water Absorption, Apparent Specific Gravity, and Bulk Density of Burned Refractory Brick and Shapes by Boiling Water, American Society for Testing and Materials, 2022.
23. Spiridonov Y. A., and Orlova L. A. - Problems of Foam Glass Production, Glass and Ceramics **60** (2003) 313-314. doi: 10.1023/B:GLAC.0000008234.79970.2c.
24. König J., Petersen R. R., and Yue Y. - Influence of the glass-calcium carbonate mixture's characteristics on the foaming process and the properties of the foam glass, Journal of the European Ceramic Society **34** (2014) 1591-1598. doi: 10.1016/j.jeurceramsoc. 2013.12.020.
25. Kilinc E., and Hand R. J. - Mechanical properties of soda-lime-silica glasses with varying alkaline earth contents, Journal of Non-Crystalline Solids **429** (2015) 190-197. doi: 10.1016/j.jnoncrysol.2015.08.013.
26. Jiusti J., Zanotto E. D., Feller S. A., Austin H. J., Detar H. M., Bishop I., Manzani, D., Nakatsuka, Y., Watanabe, Y., and Inoue, H. - Effect of network formers and modifiers on the crystallization resistance of oxide glasses, Journal of Non-Crystalline Solids **550** (2020) 120359. doi: 10.1016/j.jnoncrysol.2020.120359.
27. Kahlenberg V., Girtler D., Arroyabe E., Kaindl R., and Többens D. M. - Devitrite ($Na_2Ca_3Si_6O_{16}$)-structural, spectroscopic and computational investigations on a crystalline

impurity phase in industrial soda-lime glasses, Mineralogy and Petrology **100** (2010) 1-9. doi: 10.1007/s00710-010-0116-8.

28. Chung S. Y., Sikora P., Kim D. J., El Madawy M. E., and Abd Elrahman M. - Effect of different expanded aggregates on durability-related characteristics of lightweight aggregate concrete, Materials Characterization **173** (2021) 110907. doi:10.1016/ j.matchar.2021.110907.
29. Lauermannová A. M., Jankovský O., Sedmidubský D., Lojka M., Pavlíková M., Pivák A., Záleská M., and Pavlík Z. - Case study on MOC composites enriched by foamed glass and ground glass waste: Experimental assessment of material properties and performance, Case Studies in Construction Materials **18** (2023) e01836. doi:10.1016/ j.cscm.2023.e01836.